

pubs.acs.org/JPCA Article

Unified Description of the Jahn-Teller Effect in Molecules with Only C_s Symmetry: Cyclohexoxy in Its Full 48-Dimensional Internal Coordinates

Yifan Shen* and David R. Yarkony*



Cite This: J. Phys. Chem. A 2022, 126, 61-67



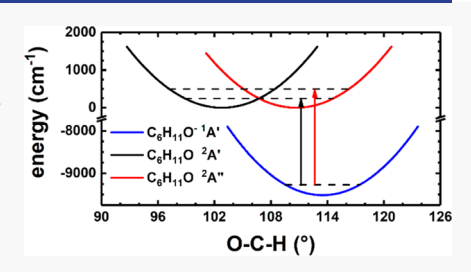
ACCESS I

Metrics & More

Article Recommendations

Supporting Information

ABSTRACT: The two lowest potential energy surfaces of cyclohexoxy which are coupled by conical intersections and the spin—orbit interaction are determined in the full 48-dimensional internal coordinate space using a feedforward neural network to fit a diabatic potential energy matrix. The electronic structure data are obtained at the multireference configuration interaction with single- and double-excitation level. Underlying parallels between these coupled surfaces and those of the alkoxy radicals methoxy and isopropoxy are established. Earlier work by Dillon and Yarkony is extended. While the parallels would have been challenging to appreciate using the concept of the Jahn—Teller active modes, they are readily seen in terms of two internal



modes centered at the conical intersection: \mathbf{g} the energy difference gradient vector and \mathbf{h} the interstate coupling gradient vector. In other words, \mathbf{g} and \mathbf{h} vectors provide a unified description of the Jahn-Teller effect in molecules exhibiting C3v and quasi-C3v symmetries. A spectral simulation in the full 48-vibrational-internal coordinate space is reported. This spectrum is obtained using recently developed algorithms designed to increase the size of the systems that can be treated with a time-independent vibronic coupling approach.

I. INTRODUCTION

The prevalence of cyclic hydrocarbons in nontraditional fuel sources such as oil shales and oil sands has stimulated interest in cyclic alkoxy radicals, ¹ which also play important roles in atmospheric chemistry, ² combustion, ³ and radiolysis. ⁴ In this work, we consider the electronic structure and the spectroscopy of cyclohexoxy ($C_6H_{11}O$). Two factors guide our understanding of the electronic structure of alkoxy radicals ($R_1R_2R_3CO$):

- (1) Alkoxy radicals are substitutional isomers of methoxy (CH₃O), one of the simplest molecules to exhibit a true symmetry-required Jahn—Teller⁵ conical intersection^{6–9} (CI), which has been the subject of a great deal of experimental and computational study. Alkoxy radicals inherit an accidental CI from methoxy.

A key quantity in this work is the (electronic) $\tilde{X}-\tilde{A}$ splitting, the separation of the two electronic states derived from the Jahn–Teller split 2E state in methoxy with the spin–orbit interaction included. When the electronic energy separation is small, molecular vibrations can couple the electronic states, so the experimentally measured $\tilde{X}-\tilde{A}$ splitting should be compared

to an $\tilde{X}-\tilde{A}$ splitting, which includes the nonadiabatic nuclear motion.

A fundamental issue addressed in this work is the size of $\tilde{X} - \tilde{A}$ splitting in alkoxy radicals. It is small (\sim 65 cm⁻¹) for methoxy (CH_3O) , isopropoxy (C_3H_7O) , 2-butoxy (C_4H_9O) , and cyclohexoxy (C₆H₁₁O), but much larger for others including ethoxy (C_2H_5O) at 355 cm⁻¹. These experimental results were obtained from cryogenically cooled slow electron velocity-map imaging (cryo-SEVI) anion photoelectron (APE) spectroscopy in Neumark's laboratory and jet-cooled laser-induced fluorescence (jet-LIF) spectroscopy in Miller's laboratory. 30-34 Dillon and Yarkony's (DY's) computational study³⁵ of C₃H₇O, a double-methyl substituted methoxy, revealed the origin of the $CH_3O-C_3H_7O$ similarity: the $\tilde{X}-\tilde{A}$ splitting in C_3H_7O is limited by its low-lying C_s ²A'-²A" CI, which retains the properties (see Section III) of a methoxy C_{3v} ²E CI being split only modestly by geometrical distortion along Jahn-Teller active modes. To further test this idea, it is important to get examples with larger spaces of Jahn-Teller active modes and determine, accurately for low energies, the APE spectra. $C_6H_{11}O$ is an excellent candidate for this analysis with its 48 internal

Received: October 20, 2021 Revised: December 11, 2021 Published: December 29, 2021





The Journal of Physical Chemistry A

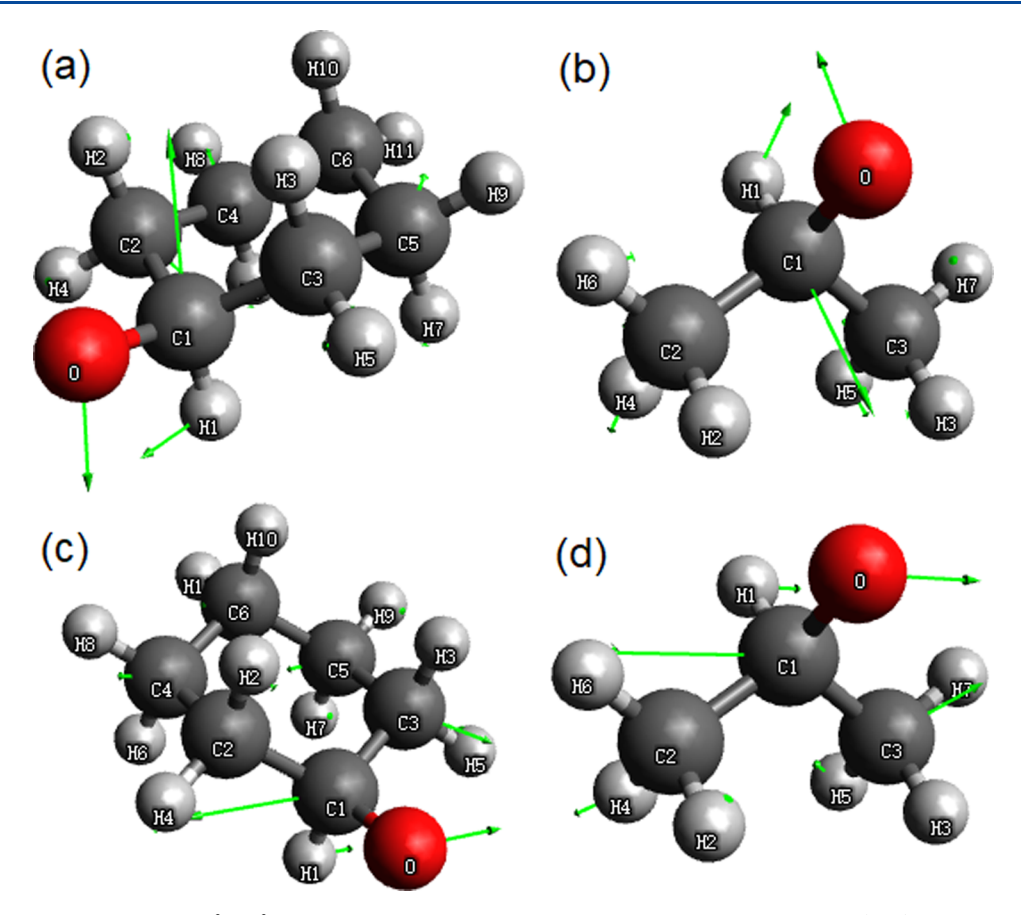


Figure 1. Cyclohexoxy and isopropoxy ${}^{2}A' - {}^{2}A''$ minimum energy conical intersection structure, along with (a, b) normalized **g**, the A' energy difference gradient vector; (c, d) normalized **h**, the A'' interstate coupling gradient vector. Isopropoxy reproduced from Dillon and Yarkony, ³⁵ with the permission of AIP Publishing.

modes, but it has not been possible to carry out requisite computations to validate this model until recent theoretical advancements. 36,37

Thus, in this work, we will investigate $C_6H_{11}O$ to understand the similarity of CH_3O , C_3H_7O , and $C_6H_{11}O$ $\tilde{X}-\tilde{A}$ splittings. The work is made challenging by the need to determine the APE spectrum for a molecule with 48 internal coordinates. It is made interesting by the use of an intersection adapted coordinate system based on g the energy difference gradient vector and h the interstate coupling gradient vector to provide a clear description of the branching and the seam spaces near a CI. The $C_3H_7O-C_6H_{11}O$ similarity will be found to extend beyond the low-energy portion of the APE spectra. Our atomistic analysis will suggest that the local topography of a CI qualitatively shape the vibronic structure despite the size of a molecule, leading to a surprising vibronic spectra resemblance.

This paper is organized as follows. Section II briefly reviews the algorithms used in this work to obtain the diabatic potential energy matrix and to construct the vibrational Schrödinger equation whose solution is used to construct the APE spectrum. Section III presents the $C_6H_{11}O$ minimum energy CI and discusses its similarity to CH_3O and C_3H_7O in molecular structure, local CI topography, and the Mexican-hat coupled potential energy surfaces. A systematic method of describing molecular coordinates in the vicinity of a CI will help to understand the quasi Jahn–Teller condition. Section III discusses the existing experimental observables: the jet-LIF spectra $^{30-34}$ and the APE spectra 27 and the comparable computational results. Section IV summarizes and discusses

future directions. The $CH_3O\left(C_3H_7O\right)$ computational data used for comparison herein are taken from Weichman et al. ¹⁹ (DY ³⁵).

II. METHODOLOGY

The vibronic spectrum simulation is accomplished in three steps. In the first step, the requisite electronic structure data is determined. The cold anion $C_6H_{11}O^-$ is described by a single-reference configuration interaction with single- and double-excitation (CISD) wave function. It is the neutral radical $C_6H_{11}O$ that exhibits the conical intersection induced non-adiabaticity, which in turn requires a multireference CISD (MRCISD) description. All electronic structure calculations in this work employ the COLUMBUS $^{40-50}$ suite of programs.

In the second step, ab initio adiabatic electronic energies, energy gradients, and derivative couplings determined in step 1 are accurately fit^{36,51,52} to a diabatic potential energy matrix (DPEM) for use in the vibrational Schrödinger equation (VSE). The elements of the two-state DPEM are expanded with quadratic polynomials of normal coordinates, consisting of 1862 parameters in total. The training set of electronic structure data contains 916 geometries, equivalent to 150 224 fitting equations. The fit is excellent with the total root mean square deviation of the energy being 7 cm⁻¹. The fitting method-based artificial intelligence concepts are described in detail in the Supporting Information.

For the third step, we use a time-independent approach, the Köppel-Domcke-Cederbaum⁵³⁻⁵⁶ (KDC) approach in which the nonrelativistic VSE is constructed on a multimode basis and solved using an iterative Lanczos procedure, to obtain

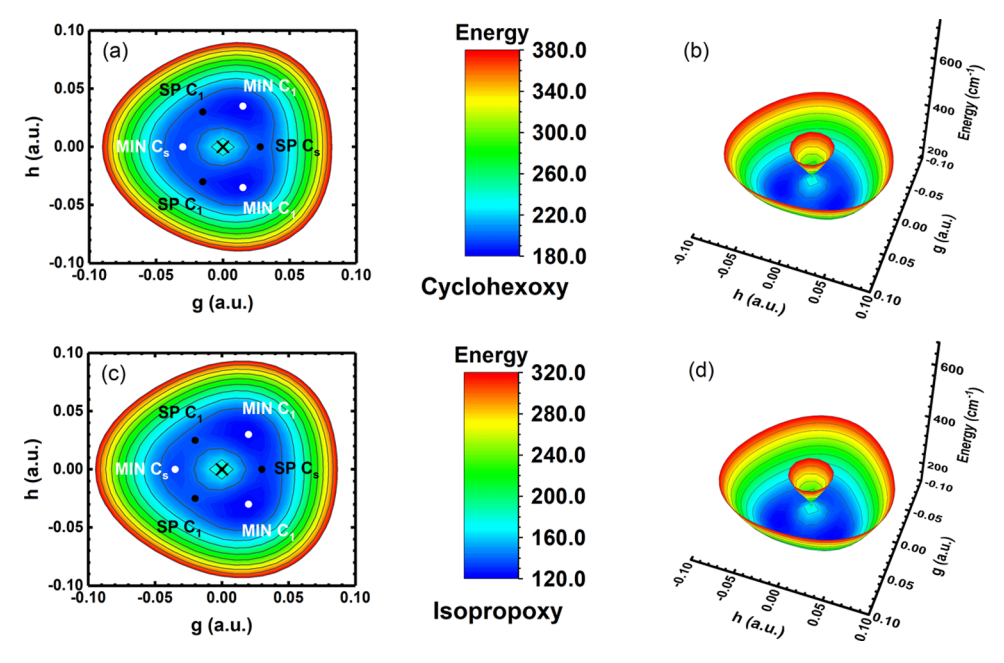


Figure 2. Within the branching plane of cyclohexoxy/isopropoxy $^2A'-^2A''$ minimum energy conical intersection (X) spanned by **g** and **h**, the (a, c) lower state surface, with X and the approximate locations of the three minima (MIN) and the three saddle points (SP) marked; (b, d) coupled surfaces illustrating the Mexican-hat topographies.

nonrelativistic vibronic wave functions. The intensities in the APE spectroscopy are also determined during the Lanczos iterations. The spin—orbit interaction is included in the spin-diabatic approximation in a truncated eigenbasis of the nonrelativistic VSE. ⁵⁷

Solving the nonrelativistic VSE is the bottleneck because the curse of dimensionality gives rise to the exponential growth of the requisite computational effort over the number of vibrational modes. The size of the systems that can be treated is increased using a continuum model 37 to help reduce the size of the space needed to solve the VSE. The convergence of the continuum-model-based approach is established by a detailed comparison to the standard energy-based approach, where both approaches converge the lowest four vibronic states as required by the E \otimes e Jahn—Teller problem, and the continuum-model-based approach outperforms the standard approach in faster convergence of the low-energy portion and the ability to give the spectral envelope. The detailed discussion can be found in the Supporting Information.

III. RESULTS AND DISCUSSION

III.I. Conical Intersections and Quasi- C_{3v} Symmetry. We now turn to the electronic structure data required to construct the DPEM. Since we will be particularly interested in the low-energy portion of the APE spectrum, we begin our study by locating the $C_6H_{11}O$ minimum energy CI also referred to as the minimum energy crossing (MEX). The MEX has C_s point group symmetry and is a symmetry-allowed $^2A'-^2A''$ CI with chair conformation and the equatorial C-O bond.

Regardless of the size of a molecule, at a CI, the coordinate system can be chosen so that the degeneracy is lifted linearly in only one plane, the \mathbf{g} — \mathbf{h}^{39} or branching³⁸ plane defined by the energy difference gradient vector \mathbf{g} , which carries the A' irreducible representation, and the interstate coupling gradient vector \mathbf{h} , which carries the A' irreducible representation. This allows us to focus on two modes when analyzing the CI and its

consequences. Thus, using a coordinate system based on \mathbf{g} and \mathbf{h} , we can consolidate the effects of the CI (see below).

We begin with the tell for the small $\hat{X}-\hat{A}$ splitting, which is obtained from $\bf g$ and $\bf h$ vectors. These vectors, with origins at the CI, are found to have norms $||{\bf g}|| = 0.0168~(0.0168)$ and $||{\bf h}|| = 0.0184~(0.0177)$ for $C_6H_{11}O~(C_3H_7O)$ in atomic units. $||{\bf g}|| = ||{\bf h}||$ is what we get for a true C_{3v} molecule. $\bf g$ and $\bf h$ of $C_6H_{11}O$ and C_3H_7O share not only similar norms but also directions: the principal component of $\bf g$ is the scissoring of O-C1-H1, while the rocking of O-C1-H1 dominates $\bf h$, as shown in Figure 1. Fully $\sim 80\%~(\sim 90\%)$ of $\bf g~(h)$ come from these methoxy internal coordinates.

In methoxy, the g and h vectors carry an E irreducible representation of C_{3v} and can be chosen to carry A' and A" irreducible representations, respectively, in the C_s subgroup. As a result, when **g** and **h** are the A' scissoring and the A" rocking of O-C1-H1 as is the case for $C_6H_{11}O$ and C_3H_7O , the A' g and the A" h in a C_s system resemble e_x and e_y , the properly symmetrized Jahn–Teller active modes in a C_{3v} system. These equivalences, which were reported for C₃H₇O by DY, are reflected in near C_{3v} energetics in the vicinity of CI. In particular, the $\tilde{X}-\tilde{A}$ splitting is small in $C_6H_{11}O$ and C_3H_7O as a consequence of it being small, actually 0 in the nonrelativistic case, for CH₃O. This observation for C₆H₁₁O is a prediction of the DY analysis, and it is important to see that the prediction survives the enormous increase in vibrational complexity. When ${\bf g}$ and ${\bf h}$ do not resemble ${\bf e}_{\rm x}$ and ${\bf e}_{\rm v}$ as is the case of ethoxy ^{14,27,30,58} (C_2H_5O) , see also the Supporting Information), the $\tilde{X}-\tilde{A}$ splitting is large, being 355 cm⁻¹ for C₂H₅O, while it is only 62 cm⁻¹ for CH₃O. Although C₂H₅O, C₃H₇O, and C₆H₁₁O are all C_s molecules, what $C_6H_{11}O$ and C_3H_7O have in common which C_2H_5O does not is the nature of mirror plane: $O-\alpha C-\alpha H$ is the mirror plane in C₆H₁₁O and C₃H₇O, while that in C₂H₅O is O-

Thus, as originally explained by DY, \mathbf{g} and \mathbf{h} vectors tell us whether the $\tilde{X}-\tilde{A}$ splitting will be large or small. Thus, it is the conical intersection that controls the size of the $\tilde{X}-\tilde{A}$ splitting. In

other words, **g** and **h** vectors of a conical intersection provide a unified description of the Jahn–Teller effect.

With the **g**-**h** determiner established, the consequent near CI topographies are of interest. Figure 2 reports the Mexican-hat coupled potential energy surfaces (CPES) of $C_6H_{11}O$ and C_3H_7O . They both have three minima and three saddle points (SPs) on the CPES: one C_s local minimum, two C_1 global minima, one C_s SP separating two C_1 minima, and two C_1 SPs separating adjacent C_s - C_1 minima. The energies of these extrema relative to the global minima can be found in Table 1. In

Table 1. Energies in ${\rm cm}^{-1}$ of Cyclohexoxy and Isopropoxy at Critical Geometries Relative to Their Ground-State Global Minima a

	cyclohexoxy		isopropoxy	
	E_1	E_2	E_1	E_2
MIN C ₁	0.00	774.28	0.00	822.10
$MIN C_s$	34.16	756.15	22.60	833.60
SP C_1	65.28	549.14	62.10	567.70
SP C_s	30.72	572.70	33.00	608.20
MEX	251.86	251.95	193.80	193.80

"These geometries are C_1 ground-state minima (MIN C_1), C_s ground-state minimum (MIN C_s), C_1 ground-state saddle points (SP C_1), C_s ground-state saddle point (SP C_s), and $^2A'-^2A''$ minimum energy crossing (MEX).

each case, the MEX is low, ~ 0.03 eV. These CPES are largely those of a C_{3v} ²E Jahn—Teller system: if the ²E description was exact, the three minima would have identical energies. This is true for both C_1 minima, although the C_s minimum is 34 cm⁻¹ (22 cm⁻¹) higher in $C_6H_{11}O$ (C_3H_7O). In addition, Mexican hats are slightly stretched along the **g** direction, as another subtle deviation from a rigorous ²E Jahn—Teller model.

The importance of the g-h plane in this analysis is emphasized in Figure 3, which reports the energies of the $1,2^2A$ states of $C_6H_{11}O$ and C_3H_7O along two coordinates

whose only requirement is that they are orthogonal to the **g** and **h** modes. The two potential energy surfaces are nested. The Mexican-hat topography is completely absent.

III.II. Spectroscopy. In this section, we will compare our calculations to two experiments: the $C_6H_{11}O$ jet-LIF spectrum, 33,34 which gives the $\tilde{X}-\tilde{A}$ splitting, and the $C_3H_7O^-$ APE spectrum, which gives the envelope of all C_3H_7O vibronic levels. The connection to the CH_3O cryo-SEVI APE experiment 13,14,19 and C_3H_7O jet-LIF experiment $^{30-32}$ is also discussed.

The jet-LIF spectroscopy features high resolution (as accurate as 1 cm $^{-1}$), so it is an appropriate choice to study the fine-structure splitting of pseudodegenerate vibronic levels. The experimental \tilde{X} – \tilde{A} splitting of $C_6H_{11}O$ is 62 cm $^{-1}$. What is the mechanism behind this splitting? From our nonrelativistic simulation, the \tilde{X} – \tilde{A} splitting is 47 cm $^{-1}$, so the spin—orbit effect must come into play. The unquenched spin—orbit constant is 69.6 cm $^{-1}$, which enlarges the nonrelativistic splitting to 70 cm $^{-1}$, in good agreement with the experiment.

The experimental $\tilde{X}-\tilde{A}$ splittings are 62/68/62 cm⁻¹ for CH₃O/C₃H₇O/C₆H₁₁O. Why are they so close? The $\tilde{X}-\tilde{A}$ splitting is a combination of fine-structure splitting, mainly determined by the p_x and the p_y atomic orbitals of oxygen and the near degeneracy of two nonrelativistic electronic states. The spin—orbit coupling is inherited from OH, so CH₃O, C₃H₇O, and C₆H₁₁O should all share a similar unquenched spin—orbit constant. Indeed, the computed (unquenched) electronic spin—orbit constants are 66.5/62.6/69.6 cm⁻¹ for CH₃O/C₃H₇O/C₆H₁₁O, very close to the ~65 cm⁻¹ in OH. $^{13,14,19,28,30-34}$ The final splittings are half of that in OH due to the Ham reduction. From the CH₃O-C₃H₇O-C₆H₁₁O conical intersection similarity discussed in Section III, the observed similarity in the vibrational overlap that constitutes the Ham factor is not too surprising.

In the APE spectroscopy simulated in this work, an electron is detached from a cold anion, so the spectrum encodes all vibronic levels of the neutral residual. Since only the C_3H_7O experimental

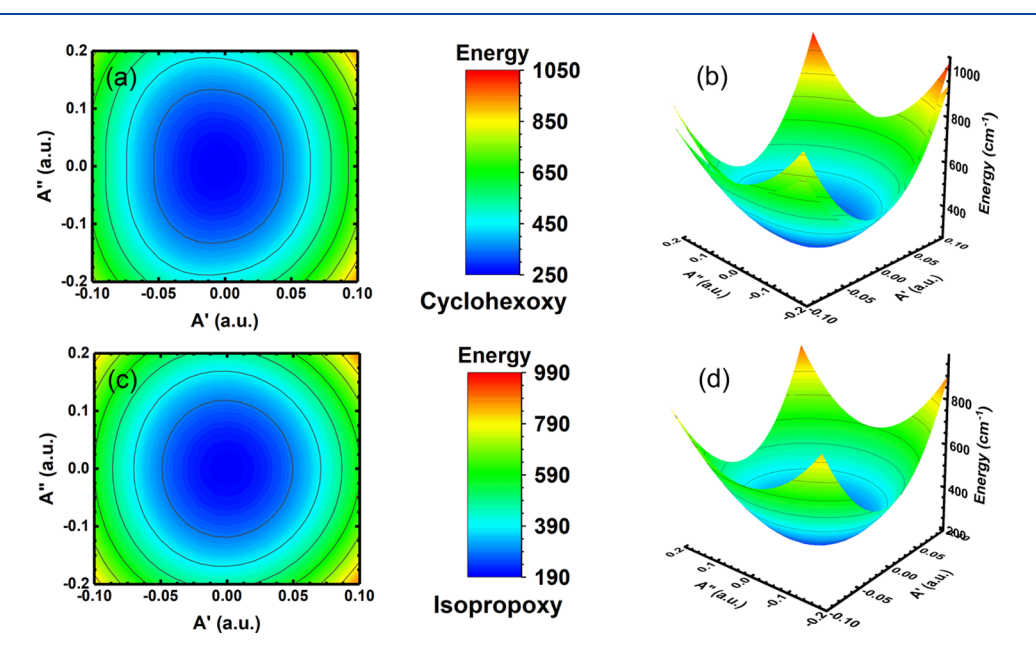


Figure 3. Arbitrary section arising from two pure seam space modes of cyclohexoxy/isopropoxy $^2A'-^2A''$ minimum energy conical intersection (MEX): (a, c) the lower state surface, with origin at the MEX; (b, d) coupled surfaces illustrating the nested potential energy surfaces and the complete absence of Mexican-hat topographies.

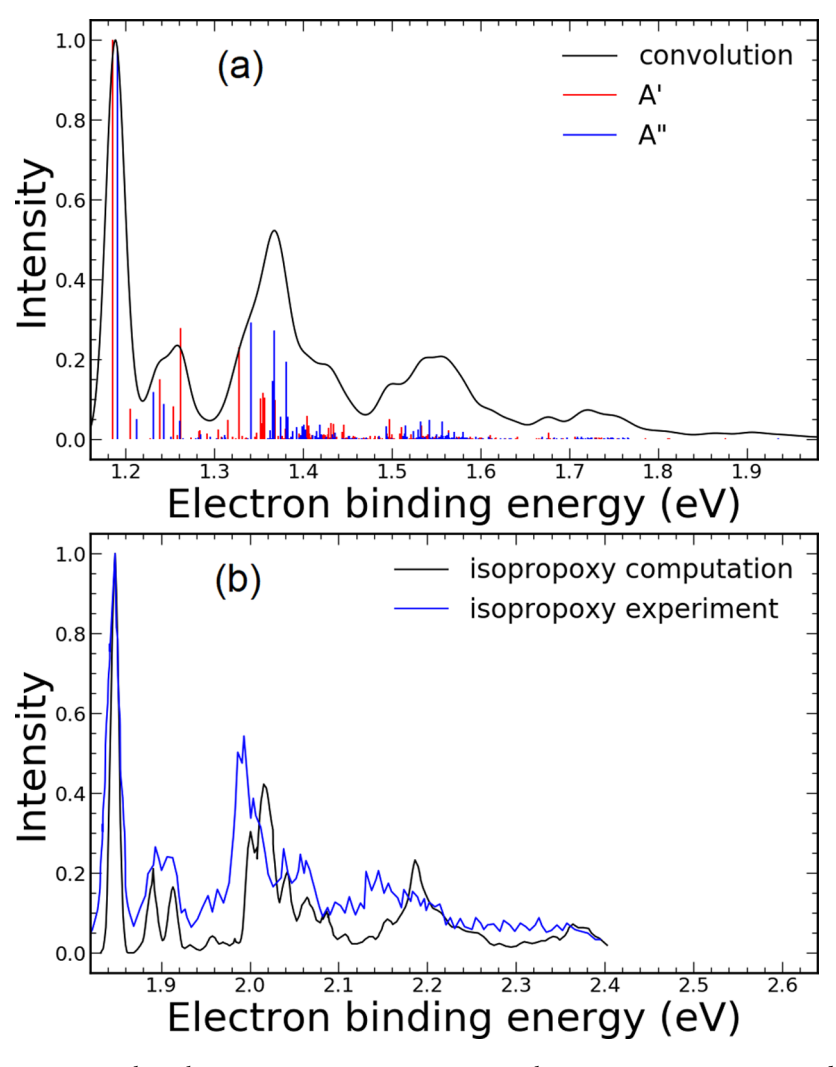


Figure 4. Simulated cyclohexoxy anion photoelectron spectrum, in comparison to the isopropoxy computation and experiment. The similarity between the spectra of these two disparate radicals is uncanny but requisite from their conical intersection similarity. Red and blue vertical lines represent the A' and the A'' vibronic levels, respectively. A Gaussian with 0.01 eV width is adopted for convolution. Isopropoxy reproduced from Dillon and Yarkony, 35 with the permission of AIP Publishing.

spectrum is available in the literature, here we study the $C_6H_{11}O$ spectrum exclusively from the computation. The quality of our $C_6H_{11}O$ computation is supported by its convergence discussed in the Supporting Information and the comparison to the jet-LIF experiment above.

Figure 4 reports the simulated $C_6H_{11}O$ spectrum and compares it to the C_3H_7O experiment. The agreement is surprising for two quite different molecules. As we can see from the spectra, they share a similar low-energy peak (the $\tilde{X}-\tilde{A}$ splittings) and the envelopes for the next peaks (position and height) are also similar. Thus, this similarity extends from the origin (discrete assignable lines) to the envelope region (where the density of the states is too large to isolate individual lines). This finding demonstrates the energetic range over which the vibronic structure is qualitatively determined from the conical intersection topography. For the higher-energy region, when compared with the C_3H_7O spectrum, the $C_6H_{11}O$ spectrum has a longer tail, resulting from a larger number of states and a higher density of states originated from the additional 21 vibrational degrees of freedom.

It would be valuable to have a measured APE spectrum for $C_6H_{11}O$. Based on the $CH_3O-C_3H_7O-C_6H_{11}O$ similarity, our

computation suggests that the locus and the local topography of a conical intersection qualitatively shape the vibronic structure despite the size of a molecule.

IV. CONCLUSIONS

To sum up, an unexpected similarity among the vibronic structures of three disparate radicals, methoxy, isopropoxy, and cyclohexoxy is found and explained. This similarity originates from their conical intersections, extends to their molecular structures, Mexican-hat coupled potential energy surfaces, and low-lying vibronic levels. For isopropoxy and cyclohexoxy, this similarity extends beyond the low-energy portion. These findings demonstrate the importance of conical intersections in shaping vibronic spectra. Our analysis suggests that not only the locus but also the local topography of the branching plane as described by the g and h vectors evince the role of conical intersections in shaping vibronic structure. In other words, g and h vectors of conical intersections provide a unified description of the Jahn-Teller effect in molecules exhibiting C3v and quasi-C3v symmetries. The spectral simulation in the full 48vibrational-internal coordinate space is empowered by our latest algorithms designed to increase the size of the systems that can

be treated with a time-independent vibronic coupling approach. In the future, additional molecules that might have similar conical intersections will be sought and studied.

ASSOCIATED CONTENT

Supporting Information

The Supporting Information is available free of charge at https://pubs.acs.org/doi/10.1021/acs.jpca.1c09123.

Details of cyclohexoxy computation: the theory and the implementation, critical geometries, the source code, and the input/output files for constructing the diabatic potential energy matrix and solving the vibrational Schrödinger equation (PDF)

AUTHOR INFORMATION

Corresponding Authors

Yifan Shen — Department of Chemistry, Johns Hopkins University, Baltimore, Maryland 21218, United States; orcid.org/0000-0003-0590-444X; Email: yifanshensz@jhu.edu

David R. Yarkony — Department of Chemistry, Johns Hopkins University, Baltimore, Maryland 21218, United States; orcid.org/0000-0002-5446-1350; Email: yarkony@jhu.edu

Complete contact information is available at: https://pubs.acs.org/10.1021/acs.jpca.1c09123

Notes

The authors declare no competing financial interest.

ACKNOWLEDGMENTS

This work was supported by the National Science Foundation grant (CHE-1954723) to D.R.Y. The authors are grateful for a grant of computer time at the Maryland Advanced Research Computing Center. The authors are grateful to Professor Lan Cheng for sharing his experience on tuning atomic orbital basis sets.

REFERENCES

- (1) Wells, G. M. Handbook of Petrochemicals and Processes; Routledge: London, 1991.
- (2) Orlando, J. J.; Tyndall, G. S.; Wallington, T. J. The Atmospheric Chemistry of Alkoxy Radicals. *Chem. Rev.* **2003**, *103*, 4657–4690.
- (3) Agarwal, A. K.; Singh, A. P.; Gupta, T.; Agarwal, R. A.; Sharma, N.; Rajput, P.; Pandey, S. K.; Ateeq, B. Mutagenicity and Cytotoxicity of Particulate Matter Emitted from Biodiesel-Fueled Engines. *Environ. Sci. Technol.* **2018**, *52*, 14496–14507.
- (4) Wargon, J. A.; Williams, E. Electron Spin Resonance Studies of Radical Trapping in the Radiolysis of Organic Liquids. I. Evidence for the Primary Formation of the Methoxy Radical in Methanol. *J. Am. Chem. Soc.* **1972**, *94*, 7917–7918.
- (5) Jahn, H. A.; Teller, E. Stability of Polyatomic Molecules in Degenerate Electronic States I. Orbital Degeneracy. *Proc. R. Soc. Lond., Ser. A* 1937, 161, 220–235.
- (6) Celani, P.; Bernardi, F.; Olivucci, M.; Robb, M. A. Conical Intersection Mechanism for Photochemical Ring Opening in Benzospiropyran Compounds. *J. Am. Chem. Soc.* **1997**, *119*, 10815–10820.
- (7) Migani, A.; Robb, M. A.; Olivucci, M. Relationship between Photoisomerization Path and Intersection Space in a Retinal Chromophore Model. *J. Am. Chem. Soc.* **2003**, *125*, 2804–2808.
- (8) Yarkony, D. R. Nonadiabatic Quantum Chemistry Past, Present, and Future. *Chem. Rev.* **2012**, *112*, 481–498.

- (9) Domcke, W.; Yarkony, D. R. Role of Conical Intersections in Molecular Spectroscopy and Photoinduced Chemical Dynamics. *Annu. Rev. Phys. Chem.* **2012**, *63*, 325–352.
- (10) Engelking, P. C.; Ellison, G. B.; Lineberger, W. C. Laser Photodetachment Electron Spectrometry of Methoxide, Deuteromethoxide, and Thiomethoxide: Electron Affinities and Vibrational Structure of CH3O, CD3O, and CH3S. *J. Chem. Phys.* **1978**, *69*, 1826–1832.
- (11) Foster, S. C.; Misra, P.; Lin, T. Y. D.; Damo, C. P.; Carter, C. C.; Miller, T. A. Free Jet-Cooled Laser-Induced Fluorescence Spectrum of Methoxy. 1. Vibronic Analysis of the \tilde{A} and \tilde{X} States. *J. Phys. Chem. A* **1988**, 92, 5914–5921.
- (12) Marenich, A. V.; Boggs, J. E. A Model Spin-Vibronic Hamiltonian for Twofold Degenerate Electron Systems: A Variational Ab Initio Study of X̃2E CH3O●. *J. Chem. Phys.* **2005**, *122*, No. 024308.
- (13) Nee, M. J.; Osterwalder, A.; Zhou, J.; Neumark, D. M. Slow Electron Velocity-Map Imaging Photoelectron Spectra of the Methoxide Anion. *J. Chem. Phys.* **2006**, *125*, No. 014306.
- (14) Neumark, D. M. Slow Electron Velocity-Map Imaging of Negative Ions: Applications to Spectroscopy and Dynamics. *J. Phys. Chem. A* **2008**, *112*, 13287–13301.
- (15) Liu, J.; Chen, M.-W.; Melnik, D.; Miller, T. A.; Endo, Y.; Hirota, E. The Spectroscopic Characterization of the Methoxy Radical. II. Rotationally Resolved Ã2A1-Ã2E Electronic and Ã2E Microwave Spectra of the Perdeuteromethoxy Radical CD3O. *J. Chem. Phys.* **2009**, 130, No. 074303.
- (16) Liu, J.; Chen, M.-W.; Melnik, D.; Yi, J. T.; Miller, T. A. The Spectroscopic Characterization of the Methoxy Radical. I. Rotationally Resolved Ã2A1–Ã2E Electronic Spectra of CH3O. *J. Chem. Phys.* **2009**, 130, No. 074302.
- (17) Shao, Z.; Mo, Y. Jahn-Teller Effect in CH2DO/CHD2O(X2E): Vibronic Coupling of All Vibrational Modes. *J. Chem. Phys.* **2013**, *138*, No. 244309.
- (18) Lee, Y.-F.; Chou, W.-T.; Johnson, B. A.; Tabor, D. P.; Sibert, E. L.; Lee, Y.-P. Infrared Absorption of CH3O and CD3O Radicals Isolated in Solid Para-H2. *J. Mol. Spectrosc.* **2015**, *310*, 57–67.
- (19) Weichman, M. L.; Cheng, L.; Kim, J. B.; Stanton, J. F.; Neumark, D. M. Low-Lying Vibronic Level Structure of the Ground State of the Methoxy Radical: Slow Electron Velocity-Map Imaging (SEVI) Spectra and Köppel-Domcke-Cederbaum (KDC) Vibronic Hamiltonian Calculations. *J. Chem. Phys.* **2017**, *146*, No. 224309.
- (20) Geers, A.; Kappert, J.; Temps, F.; Sears, T. J. Stimulated Emission Pumping Spectroscopy of CH3O (X2E, \(\nu\eta\)): New Observations on the Jahn—Teller Effect. *J. Chem. Phys.* **1993**, *98*, 4297—4300.
- (21) Misra, P.; Zhu, X.; Hsueh, C.-Y.; Halpern, J. B. Laser Excitation and Emission Spectroscopy of the Methoxy Radical in a Supersonic Jet. *Chem. Phys.* **1993**, *178*, 377–385.
- (22) Lee, Y.; Wann, G.; Lee, Y. Vibronic Analysis of the $\tilde{A} \rightarrow \tilde{X}$ Laser-induced Fluorescence of Jet-cooled Methoxy (CH3O) Radical. *J. Chem. Phys.* **1993**, *99*, 9465–9471.
- (23) Geers, A.; Kappert, J.; Temps, F.; Wiebrecht, J. W. Rotation–Vibration State Resolved Unimolecular Dynamics of Highly Vibrationally Excited CH3O (X2E). I. Observed Stimulated Emission Pumping Spectra. *J. Chem. Phys.* **1994**, *101*, 3618–3633.
- (24) Osborn, D. L.; Leahy, D. J.; Neumark, D. M. Photodissociation Spectroscopy and Dynamics of CH3O and CD3O. *J. Phys. Chem. A* **1997**, *101*, 6583–6592.
- (25) Osborn, D. L.; Leahy, D. J.; Kim, E. H.; de Beer, E.; Neumark, D. M. Photoelectron Spectroscopy of CH3O- and CD3O-. *Chem. Phys. Lett.* **1998**, 292, 651–655.
- (26) Höper, U.; Botschwina, P.; Köppel, H. Theoretical Study of the Jahn–Teller Effect in X2E CH3O. *J. Chem. Phys.* **2000**, *112*, 4132–4142.
- (27) Ramond, T. M.; Davico, G. E.; Schwartz, R. L.; Lineberger, W. C. Vibronic Structure of Alkoxy Radicals via Photoelectron Spectroscopy. *J. Chem. Phys.* **2000**, *112*, 1158–1169.
- (28) Huber, K. P.; Herzberg, G. Molecular Spectra and Molecular Structure IV: Constants of Diatomic Molecules; Van Nostrand Reinhold: New York, 1979.

- (29) Ham, F. S. Dynamical Jahn-Teller Effect in Paramagnetic Resonance Spectra: Orbital Reduction Factors and Partial Quenching of Spin-Orbit Interaction. *Phys. Rev.* **1965**, *138*, No. A1727.
- (30) Jin, J.; Sioutis, I.; Tarczay, G.; Gopalakrishnan, S.; Bezant, A.; Miller, T. A. Dispersed Fluorescence Spectroscopy of Primary and Secondary Alkoxy Radicals. *J. Chem. Phys.* **2004**, *121*, 11780–11797.
- (31) Liu, J.; Melnik, D.; Miller, T. A. Rotationally Resolved $\tilde{B} \leftarrow \tilde{X}$ Electronic Spectra of the Isopropoxy Radical: A Comparative Study. *J. Chem. Phys.* **2013**, *139*, No. 094308.
- (32) Chhantyal-Pun, R.; Roudjane, M.; Melnik, D. G.; Miller, T. A.; Liu, J. Jet-Cooled Laser-Induced Fluorescence Spectroscopy of Isopropoxy Radical: Vibronic Analysis of B-X and B-A Band Systems. *J. Phys. Chem. A* **2014**, *118*, 11852–11870.
- (33) Zu, L.; Liu, J.; Tarczay, G.; Dupré, P.; Miller, T. A. Jet-Cooled Laser Spectroscopy of the Cyclohexoxy Radical. *J. Chem. Phys.* **2004**, 120, 10579–10593.
- (34) Liu, J.; Miller, T. A. Jet-Cooled Laser-Induced Fluorescence Spectroscopy of Cyclohexoxy: Rotational and Fine Structure of Molecules in Nearly Degenerate Electronic States. *J. Phys. Chem. A* **2014**, *118*, 11871–11890.
- (35) Dillon, J. J.; Yarkony, D. R. The Photoelectron Spectrum of the Isopropoxide Anion: Nonadiabatic Effects Due to Conical Intersections and the Spin-Orbit Interaction. *J. Chem. Phys.* **2009**, *130*, No. 154312.
- (36) Shen, Y.; Yarkony, D. R. Construction of Quasi-Diabatic Hamiltonians That Accurately Represent Ab Initio Determined Adiabatic Electronic States Coupled by Conical Intersections for Systems on the Order of 15 Atoms. Application to Cyclopentoxide Photoelectron Detachment in the Full 39 Degrees of Freedom. *J. Phys. Chem. A* 2020, 124, 4539–4548.
- (37) Shen, Y.; Yarkony, D. R. Compact Bases for Vibronic Coupling in Spectral Simulations: The Photoelectron Spectrum of Cyclopentoxide in the Full 39 Internal Modes. *J. Phys. Chem. Lett.* **2020**, *11*, 7245–7252.
- (38) Atchity, G. J.; Xantheas, S. S.; Ruedenberg, K. Potential Energy Surfaces near Intersections. *J. Chem. Phys.* **1991**, *95*, 1862–1876.
- (39) Yarkony, D. R. On the Adiabatic to Diabatic States Transformation near Intersections of Conical Intersections. *J. Chem. Phys.* **2000**, *112*, 2111–2120.
- (40) Shepard, R. Geometrical Energy Derivative Evaluation with MRCI Wave Functions. *Int. J. Quantum Chem.* **1987**, 31, 33–44.
- (41) Shepard, R.; Lischka, H.; Szalay, P. G.; Kovar, T.; Ernzerhof, M. A General Multireference Configuration Interaction Gradient Program. *J. Chem. Phys.* **1992**, *96*, 2085–2098.
- (42) Mai, S.; Müller, T.; Plasser, F.; Marquetand, P.; Lischka, H.; González, L. Perturbational Treatment of Spin-Orbit Coupling for Generally Applicable High-Level Multi-Reference Methods. *J. Chem. Phys.* **2014**, *141*, No. 074105.
- (43) Shepard, R. *Modern Electronic Structure Theory Part I*; In Yarkony, D. R., Ed.; World Scientific: Singapore, 1995.
- (44) Lischka, H.; Shepard, R.; Pitzer, R. M.; Shavitt, I.; Dallos, M.; Müller, T.; Szalay, P. G.; Seth, M.; Kedziora, G. S.; Yabushita, S.; et al. High-Level Multireference Methods in the Quantum-Chemistry Program System COLUMBUS: Analytic MR-CISD and MR-AQCC Gradients and MR-AQCC-LRT for Excited States, GUGA Spin—Orbit CI and Parallel CI Density. *Phys. Chem. Chem. Phys.* **2001**, *3*, 664—673.
- (45) Lischka, H.; Dallos, M.; Shepard, R. Analytic MRCI Gradient for Excited States: Formalism and Application to the $n-\Pi^*$ Valence- and $n-\Pi^*$ Valence- and $n-\Pi^*$ Valence- and $n-\Pi^*$ Rydberg States of Formaldehyde. *Mol. Phys.* **2002**, *100*, 1647–1658.
- (46) Dallos, M.; Lischka, H.; Shepard, R.; Yarkony, D. R.; Szalay, P. G. Analytic Evaluation of Nonadiabatic Coupling Terms at the MR-CI Level. II. Minima on the Crossing Seam: Formaldehyde and the Photodimerization of Ethylene. *J. Chem. Phys.* **2004**, *120*, 7330–7339.
- (47) Lischka, H.; Dallos, M.; Szalay, P. G.; Yarkony, D. R.; Shepard, R. Analytic Evaluation of Nonadiabatic Coupling Terms at the MR-CI Level. I. Formalism. *J. Chem. Phys.* **2004**, *120*, 7322–7329.
- (48) Lischka, H.; Müller, T.; Szalay, P. G.; Shavitt, I.; Pitzer, R. M.; Shepard, R. Columbus a Program System for Advanced Multi-

- reference Theory Calculations. WIREs Comput. Mol. Sci. 2011, 1, 191–199.
- (49) Lischka, H.; Shepard, R.; Shavitt, I.; Pitzer, R. M.; Dallos, M.; Müller, T.; Szalay, P. G.; Brown, F. B.; Ahlrichs, R.; Böhm, H. J. et al. COLUMBUS, an Ab Initio Electronic Structure Program, Release 7.0, 2017.
- (50) Yabushita, S.; Zhang, Z.; Pitzer, R. M. Spin-Orbit Configuration Interaction Using the Graphical Unitary Group Approach and Relativistic Core Potential and Spin-Orbit Operators. *J. Phys. Chem.* A 1999, 103, 5791–5800.
- (51) Schuurman, M. S.; Yarkony, D. R. On the Vibronic Coupling Approximation: A Generally Applicable Approach for Determining Fully Quadratic Quasidiabatic Coupled Electronic State Hamiltonians. *J. Chem. Phys.* **2007**, *127*, No. 094104.
- (52) Papas, B. N.; Schuurman, M. S.; Yarkony, D. R. Determining Quasidiabatic Coupled Electronic State Hamiltonians Using Derivative Couplings: A Normal Equations Based Method. *J. Chem. Phys.* **2008**, 129, No. 124104.
- (53) Köppel, H.; Domcke, W.; Cederbaum, L. S. Multimode Molecular Dynamics Beyond the Born-Oppenheimer Approximation. In *Advances in Chemical Physics*; Wiley, 1984; Vol. 57, pp 59–246.
- (54) Pacher, T.; Cederbaum, L. S.; Köppel, H. Adiabatic and Quasidiabatic States in a Gauge Theoretical Framework. In *Advances in Chemical Physics*; Wiley, 1993; Vol. 84, pp 293–391.
- (55) Köppel, H.; Döscher, M.; Bâldea, I.; Meyer, H.-D.; Szalay, P. G. Multistate Vibronic Interactions in the Benzene Radical Cation. II. Quantum Dynamical Simulations. *J. Chem. Phys.* **2002**, *117*, 2657–2671.
- (56) Köppel, H.; Domcke, W.; Cederbaum, L. S. Conical Intersections; In Domcke, W.; Yarkony, D. R., Eds.; World Scientific: New Jersey, 2004
- (57) Schuurman, M. S.; Weinberg, D. E.; Yarkony, D. R. On the Simulation of Photoelectron Spectra in Molecules with Conical Intersections and Spin-Orbit Coupling: The Vibronic Spectrum of CH3S. J. Chem. Phys. 2007, 127, No. 104309.
- (58) Dillon, J. J.; Yarkony, D. R. The Photoelectron Spectrum of the Ethoxide Anion: Conical Intersections, the Spin-Orbit Interaction, and Sequence Bands. *J. Chem. Phys.* **2009**, *131*, No. 134303.